Bulletin of the Earthquake
Research Institute
Vol. 44 (1966), pp. 919-938

48. A Least Squares Method for the Focal Mechanism Determination from S Wave Data; Part II Applied Examples and Statistical Discussions.*

By Tomowo Hirasawa,

Geophysical Institute, Faculty of Science, The University of Tokyo.

(Read July 20, 1965.—Received June 29, 1966.)

Abstract

The method of least squares for the focal mechanism determination presented in Part I is successfully applied to 9 deep and intermediate earthquakes which occurred in the region of Japan.

It is concluded by means of a statistical test for the goodness of fit that a set of the residuals of the polarization angles can be regarded as a sample from a normal population. It follows that the estimates obtained by the proposed method are the maximum likelihood estimates. The fault plane solutions for the 9 earthquakes determined from the S wave data alone show satisfactory agreements with the P wave observations. It justifies the double couple hypothesis which was assumed in deriving the least squares method.

1. Introduction

In the first paper (Part I) a least squares method for the focal mechanism determination has been presented by use of S wave data, where the sum of squares of the residuals of the polarization angles is minimized. Main purposes in the present paper are as follows:

1. To estimate characteristics of population distribution of the observations (the residuals of the polarization angles).
2. To examine efficiency of the least squares method given in the previous paper for various sizes of samples of the observations.
3. To examine consistency of the fault plane solution determined from the S wave data alone with the observations of P waves, in other words, to justify the hypothesis of double couple in the study of focal mechanisms assumed in derivation of the analytical method.
4. To ascertain the known pattern of the pressure directions oriented

* Communicated by H. Honda.

systematically in and near Japan by use of the solutions purely independent of the P wave data.

It depends upon characteristics of the observations whether the solution obtained by means of the least squares method is the maximum likelihood solution or not. It may be naturally expected that deviations of observed polarization angles from theoretical ones are sampled from a population of the normal distribution, and the results given by Stauder and Bollinger (1964) may support the assumption of the normal population in practical rigorousness. In this paper the assumption will be justified by use of a statistical test, and it will be shown that the method is not a merely expedient one.

First, three examples of deep focus earthquakes will be presented. The data of the polarization angle for the three shocks have been obtained by the present author as one of co-workers, and it may be expected that the data are obtained by uniform processing. Using these earthquakes, therefore, discussions on the first purpose stated above will be made. Next, for six earthquakes fault plane solutions from the S wave data, which have been given by Ritsema (1965), will be discussed in connection with the other purposes. Hypocentral coordinates and origin times (GMT) for these earthquakes are listed in Table 1.

Table 1. Earthquakes chosen for the analysis

Date	Time	Latitude	Longitude	Depth
	h m s			
1935, May 31	08 19 —	38.7° N	134.0° E	0.07 R
1952, Oct. 26	08 41 —	34.1	137.8	0.04
1956, Feb. 18	07 34 19	30.0	138.5	0.07
1934, June 13	01 51 01	44.2	147.4	0.01
1951, July 11	18 21 51	28.1	139.9	0.07
1954, May 14	22 39 25	36.0	137.4	0.03
1957, Jan. 3	12 48 27	44.0	130.0	0.09
1960, Oct. 8	05 53 01	40.0	129.7	0.09
1961, Jan. 16	07 20 19	36.0	141.0	0.01

2. Fault Plane Solutions for Three Deep Focus Earthquakes

For the first three deep focus earthquakes in Table 1 the observed polarization angle is approximated by $\tan^{-1}(\bar{u}_H/\bar{u}_R)$, where $\bar{u}_R$ and $\bar{u}_H$,

respectively, are the components along and perpendicular to the great circle path at the station, of the linear particle motion diagram of the horizontal surface motion produced by the incidence of S wave. The data and graphical solutions for the 1935 and 1952 shocks have been presented by H. Honda, M. Ichikawa, and T. Hirasawa at the annual meeting of the Seismological Society of Japan in 1962.

Table 2. S wave data for the earthquake of May 31, 1935

	Δ	α_S	i_d	α_E	Γ
Toyooka	3.°2	168.°4	137.°8	167.°9	−53.°2
Toyama	3.2	128.5	137.5	126.5	−91.5
Hikone	3.8	152.5	131.4	151.3	−86.1
Nagano	3.9	122.3	131.0	119.7	−74.6
Kyoto	3.9	159.9	130.8	158.9	−48.4
Gifu	3.9	146.9	130.6	145.2	−68.7
Hamada	4.1	201.5	129.2	−157.4	−49.2
Kobe	4.1	166.9	129.0	166.2	−67.1
Kameyama	4.3	153.3	127.2	151.8	−72.8
Sumoto	4.4	170.7	126.2	170.1	−61.7
Hiroshima	4.5	195.9	125.3	−163.2	−48.3
Wakayama	4.5	168.4	124.8	167.7	−57.4
Kofu	4.7	130.8	123.2	128.1	−82.9
Akita	4.9	79.5	121.9	75.6	79.5
Matsuyama	4.9	191.2	121.3	−168.1	−68.3
Kochi	5.1	184.1	119.6	−175.6	−60.9
Omaezaki	5.3	141.3	118.3	138.8	−105.7
Mishima	5.3	133.2	118.0	130.3	−61.7
Shionomisaki	5.4	165.2	117.3	164.1	−48.1
Tsukubasan	5.4	118.5	117.1	114.8	−13.9
Kakioka	5.5	118.1	116.5	114.4	−10.7
Zinsen	5.9	256.2	113.2	−99.2	128.8
Dairen	9.7	267.5	94.0	−84.8	140.7
Nemuro	9.9	65.9	92.8	58.3	91.6

Δ: Epicentral distance.
α_S: Azimuth of the great circle path with respect to the station.
i_d: Angle of incidence at the focus.
α_E: Azimuth of the great circle path with respect to the epicenter.
Γ: Observed polarization angle.

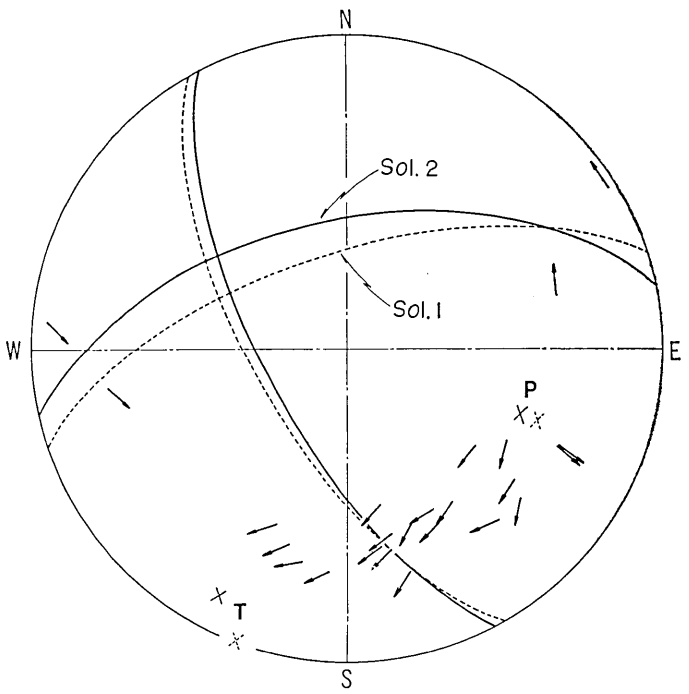

	Dip Direc.	Dip	Dip Direc.	Dip
Sol. 1	162°	65°	60°	66°
Sol. 2	167.9±2.8	56.3±6.0	62.2±2.3	67.9±3.7

Fig. 1. The radiation pattern of the observed *S* waves for the earthquake of May 31, 1935.

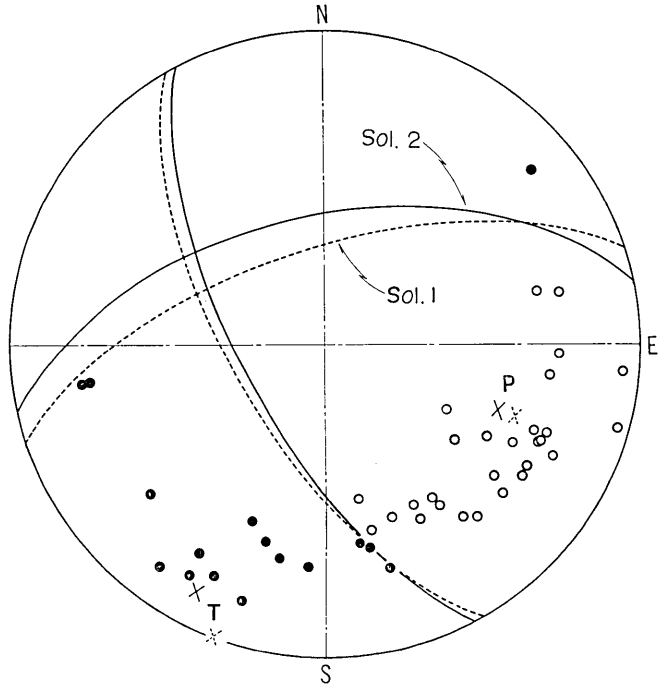

Fig. 2. The radiation pattern of the observed *P* waves for the earthquake of May 31, 1935.
The open and solid circles are rarefactions and compressions, respectively.

The crosses with the letters **P** and **T** indicate the pressure and tension axes, respectively, where the axes appropriate for a solution should be distinguished from two solutions by solid or dotted line segments. For Figures 1 to 6, the observed *S* or *P* motion is illustrated by the equal area projection of the upper hemisphere, and the solution 1 and solution 2 in the figures correspond to the graphical solution and the least squares solution, respectively.

Earthquake of May 31, 1935

The S wave data are tabulated in Table 2. The pattern of motion directions of the observed S wave is shown in Figure 1, where the upper half of the focal sphere is projected by use of the equal area net. The number of observations (N) amounts to 24. Solution (1) in the figure is the graphical solution previously obtained mainly from the P wave observations and solution (2) is the present least squares solution from the S wave data alone. The cross signs with the letters, **P** and **T**, in the figure show locations of the pressure and tension axes on the focal sphere, where the cross signs of solid and dotted lines correspond to solution (1) and solution (2), respectively. The estimated standard deviation of the observations (polarization angles) is 16°.9, which will be abbreviated by *ESD* hereafter. The most probable values of dip directions and dip angles of two P-nodal planes are also presented together with their standard deviations in the figure.

It is seen in Figure 2 that the L.S. solution surprisingly satisfies the distribution of compression-rarefaction of the observed P waves.

Earthquake of October 26, 1952

The S wave data are tabulated in Table 3. Figure 3 shows the pattern of the observed S wave motions and the graphical solution (1) obtained previously and the L.S. solution (2), where $N=35$ and $ESD=22°.0$. In the figure a comparatively large number of S wave observations are located on the points near each of the two nodal planes of the P wave, and it is found that the standard deviation of the dip angle is large compared with that of the dip direction. From Figure 4 it is seen that the graphical solution obtained mainly from the P wave data does not explain the observed P wave data better than the L. S. solution from the S wave data alone.

Earthquake of February 18, 1956

This earthquake which occurred south of Honshu, Japan, has been analyzed by many investigators. Above all, Honda (1962), Kasahara (1963), Hirasawa and Stauder (1964), and Ritsema (1965) studied independently the radiation pattern of the S waves by means of various methods of the analysis and confirmed more or less that the earthquake can be explained by the double couple hypothesis. The ample data for

Table 3. S wave data for the earthquake of October 26, 1952

	Δ	α_s	i_d	α_E	Γ
Omaezaki	0.°6	33.°3	169.°0	32.°3	78.°5
Shizuoka	1.0	29.7	156.5	28.9	118.2
Tsu	1.2	299.4	153.4	−60.0	−48.1
Nagoya	1.3	327.0	152.6	−32.8	9.2
Owashi	1.3	268.0	151.4	−91.0	−114.5
Kameyama	1.3	304.0	151.4	−55.1	−50.1
Mishima	1.4	42.6	150.8	41.9	84.0
Oshima	1.5	63.7	148.8	62.9	105.1
Gifu	1.5	326.4	147.2	−32.9	−23.1
Funatsu	1.6	29.2	146.5	28.6	80.9
Kofu	1.7	22.2	145.1	22.0	66.9
Shionomisaki	1.8	248.6	142.7	−110.3	149.0
Tomisaki	1.9	64.5	141.7	63.5	145.2
Kyoto	1.9	297.5	140.2	−61.3	−107.5
Hachijo-jima	1.9	121.6	140.2	120.5	−122.7
Osaka	1.9	285.7	139.9	−73.0	−132.0
Yokohama	2.0	49.4	138.3	48.5	−102.3
Tsuruga	2.1	317.0	137.4	−42.0	−54.2
Matsumoto	2.1	3.8	136.7	3.7	60.6
Chichibu	2.2	29.5	136.5	28.8	73.3
Kobe	2.2	284.4	135.3	−74.1	−138.2
Sumoto	2.4	274.8	132.9	−83.6	−124.1
Maizuru	2.4	303.8	132.6	−54.8	−109.1
Himeji	2.7	285.1	129.4	−73.1	−139.9
Toyooka	2.8	299.6	127.4	−58.7	−109.7
Kakioka	2.9	43.6	126.6	42.2	85.1
Utsunomiya	3.0	35.1	125.8	34.0	98.4
Choshi	3.0	57.9	125.6	56.1	108.7
Takamatsu	3.1	273.0	124.5	−84.8	−127.8
Tottori	3.3	294.3	122.4	−63.6	−131.5
Kochi	3.6	260.1	119.3	−97.5	125.3
Matsuyama	4.2	265.1	113.8	−92.1	160.6
Saigo	4.2	298.7	113.6	−58.8	−130.3
Fukushima	4.2	31.6	113.4	30.1	72.3
Shimizu	4.3	250.6	113.4	−106.8	84.8

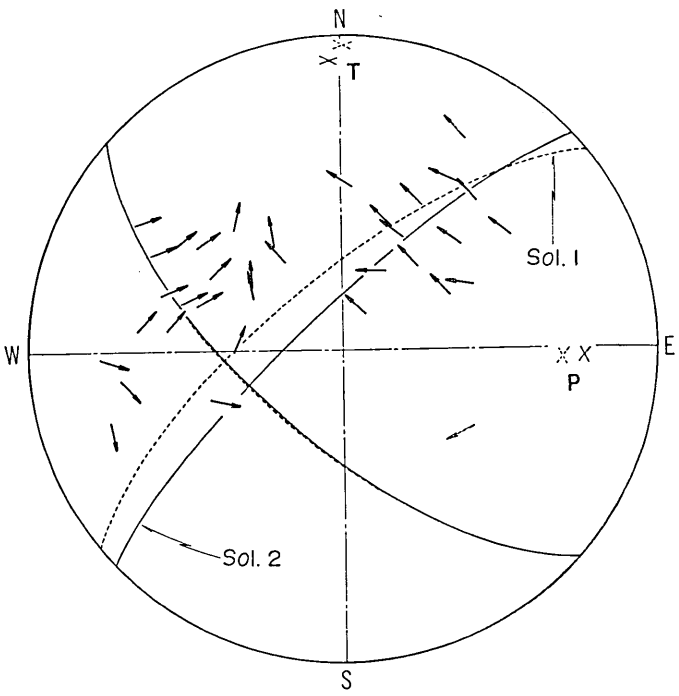

	Dip Direc.	Dip	Dip Direc.	Dip
Sol. 1	141°	71°	42°	66°
Sol. 2	136.8±2.8	79.0±3.4	42.0±2.5	66.7±4.0

Fig. 3. The radiation pattern of the observed S waves for the earthquake of Oct. 26, 1952.

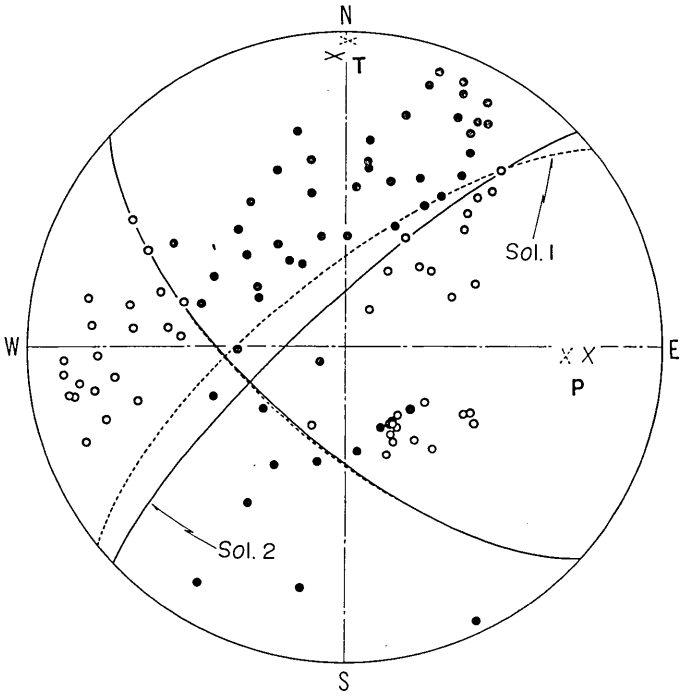

Fig. 4. The radiation pattern of the observed P waves for the earthquake of Oct. 26, 1952.

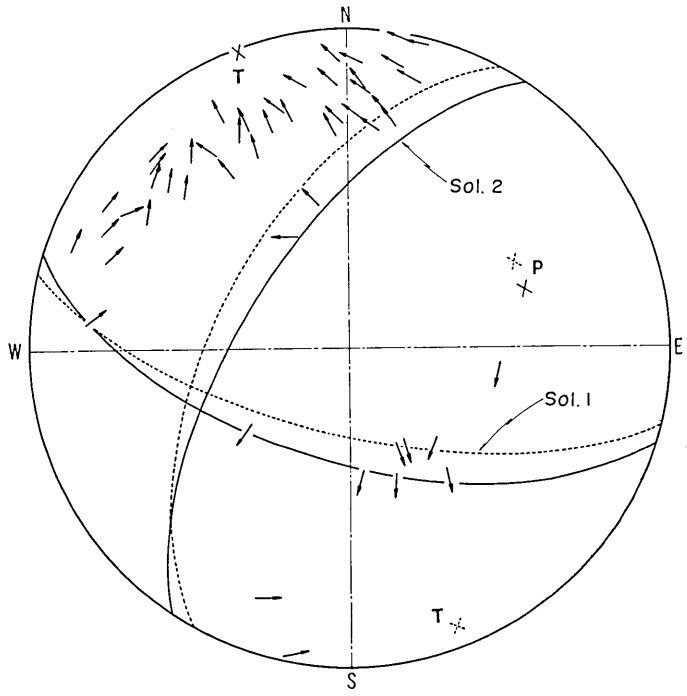

	Dip Direc.	Dip	Dip Direc.	Dip
Sol. 1	119°	56°	14°	68°
Sol. 2	123.9±2.9	63.1±2.6	17.4±2.0	60.8±3.5

Fig. 5. The radiation pattern of the observed *S* waves for the earthquake of Feb. 18, 1956.

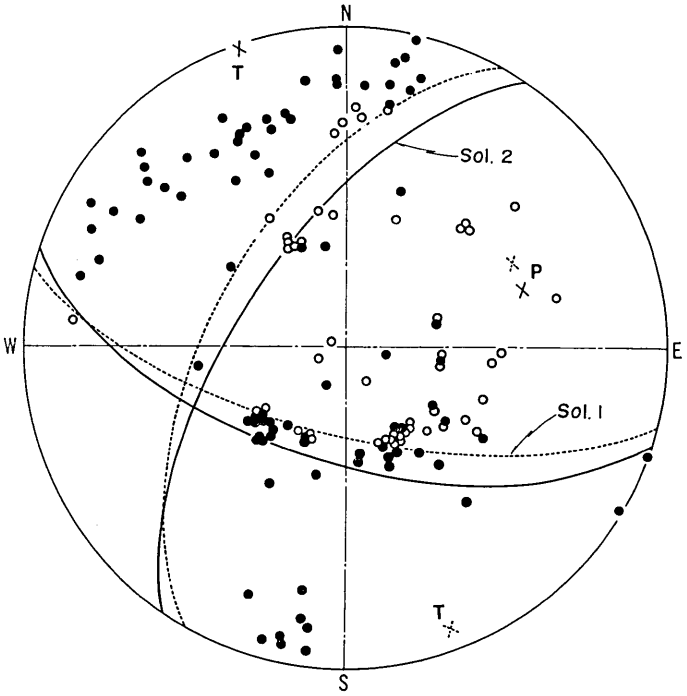

Fig. 6 The radiation pattern of the observed *P* waves for the earthquake of Feb. 18, 1956.

the S wave used here has been presented by Honda *et al.* (1965), indeed the number of observations of the S wave amounts to 50. Figure 5 shows the observations of the S wave, where solution (1) is the graphical solution given by Honda *et al.* (1965) and solution (2) is the L.S. solution determined by using the fifty observations. The *ESD* is calculated to be 16°.9. Figure 6 illustrates the observations of the P wave, and it may

Table 4. Fault plane solutions with standard deviations*

		1935, May 31		1952, Oct. 26		1956, Feb. 18	
(N)		24		35		50	
$\left(\sum_j \left(\frac{\partial \Psi}{\partial x_j'}\right)^2\right)$		6.5×10^{-10}		1.5×10^{-10}		7.7×10^{-11}	
$\left(\sum_j \varepsilon_j^2\right)$		1.5×10^{-12}		7.5×10^{-12}		4.2×10^{-14}	
(x_1')		1.46765		−1.72461		−1.70420	
(x_2')		−0.31442		−1.55347		−0.53346	
(x_3')		−0.45845		−0.28471		−0.61003	
(V_{11})		1.18513		0.94195		0.62443	
(V_{22})		0.20507		0.47578		0.16907	
(V_{33})		0.09576		0.05565		0.08044	
(V_{12})		−0.45766		0.61598		0.28940	
(V_{13})		−0.25416		0.08147		−0.08354	
(V_{23})		0.09319		0.05065		−0.03791	
S. S. Res. in rad^2	(Ψ)	1.82010		4.73456		4.10559	
Variance in rad^2	$(\hat{\sigma}^2)$	0.08667		0.14795		0.08735	
Standard Deviation	$(\hat{\sigma})$	16°.9		22°.0		16°.9	
Average of Residuals	$(\overline{R})$	−1°.9		−2°.5		4°.2	
Nodal Plane (a)	Dip Direc.	167°.9	±2°.8	42°.0	±2°.5	17°.4	±2°.0
	Dip Angle	56.3	6.0	66.7	4.0	60.8	3.5
Nodal Plane (b)	Dip Direc.	62.2	2.3	136.8	2.8	123.9	2.9
	Dip Angle	67.9	3.7	79.0	3.4	63.1	2.6
Pressure Axis	Trend	−69.0	2.6	−88.5	3.3	−108.5	2.1
	Plunge	41.1	3.0	24.5	2.9	41.7	4.1
Tension Axis	Trend	27.4	3.8	177.7	2.2	160.1	2.0
	Plunge	7.3	5.6	8.3	4.2	1.5	2.3
Null Axis	Trend	125.5	4.2	70.3	6.8	68.5	4.2
	Plunge	47.9	7.1	63.9	4.6	48.3	6.8
Slip Angle	Plane (a)	26.9	3.3	12.0	3.5	31.2	3.6
	Plane (b)	36.8	8.9	23.8	5.2	33.2	4.4

*In regard to the notations used above the previous paper is referred to.

be seen that the P wave observations can be explained fairly well by the L.S. solution.

The least squares solutions obtained above are listed in detail in Table 4. Making use of the numerical values of x_j' and V_{ij} in the table and of equations (22) and (23) in the first paper, the standard deviation for any quantity being a function of x_j' is obtainable. No minimum has been found in all the cases of the three shocks other than the solutions presented here.

3. Statistical Discussions

It seems that the above three earthquakes are suitable for the purpose of this section because of comparatively large sizes of the samples, unified

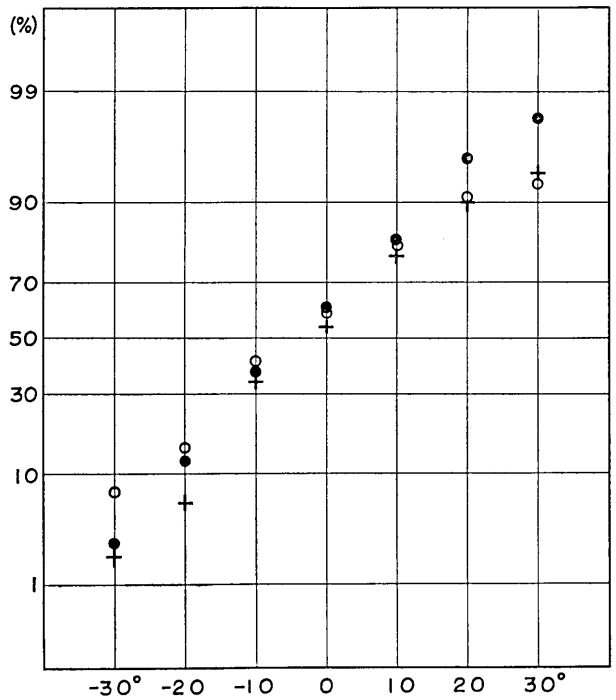

Fig. 7. The cumulative frequency distribution on a normal probability paper.

The crosses indicate cumulative frequencies of the sample of the residuals for the shock of 1956, solid circles those of the superposed sample from the shocks of 1956 and 1935, and open circles those from three shocks (1956, 1935, and 1952).

processing in deriving polarization angles, and satisfactory agreements of the L.S. solutions with the results from the P waves. Especially in case of the earthquake of 1956, size of the sample of the polarization angle seems to be largest among those for many earthquakes for which the S wave data have been published. Nevertheless the size is not sufficient enough to estimate its population distribution directly from the frequency distribution of the sample. For this purpose, therefore, a statistical test for the goodness of fit may be appropriate in the case of this earthquake. By making use of the χ^2-test, the hypothesis that the set of the observations is sampled from a population of the normal distribution is tested, where the observations mean deviations of observed polarization angles from theoretically expected ones. Even if the level of significance is taken to be 0.10, the hypothesis cannot be rejected. Now the set of the observations in the case of the 1956 shock may be regarded as a sample from a population of the normal distribution. Crosses in Figure 7 indicate cumulative frequencies in percentage plotted on a normal probability paper, of the sample for the 1956 shock ($N=50$).

In the cases of the other two shocks, sizes of the samples are not sufficiently large even for the χ^2-test. Assuming that the observations for both the 1956 and 1935 shocks are sampled from the same population, a cumulative frequency distribution of the superimposed sample ($N=74$) is indicated by solid circles in the same figure as before. By the linearity of the sample distribution on the probability paper, the assumption may be practically justified.

Next, the observations from all of the three shocks are superposed in the same way as was done above to give a sample frequency distribution shown by open circles in the figure, where $N=109$. In spite of the larger size of the sample in the latter case, the linearity is worse than in the former. However, it does not necessarily follow that the assumption of normal distribution is wrong. It is perhaps attributed to difference of the population variance for the 1952 shock from those for the others. In fact, estimates of population variances for the 1935 and 1956 shocks are practically the same, while the estimate for the 1952 shock is apparently larger than those for the others. The statistical test by means of the F-distribution shows that the difference of the estimates of the population variances is significant in the 5% limit of significance.

It may be naively expected that a set of the observations is a sample from a population of the normal distribution in general, though the above result does not necessarily assure in strict sense validity of

the assumption of the normal distribution for an individual of the three earthquakes separately except in the case of the 1956 shock. Thus, the estimate obtained by the present method of the least squares can be regarded as the maximum likelihood estimate.

4. Further Examples of Numerical Solutions

Six more numerical examples of the fault plane soultions are given chiefly with regard to the last three purposes stated in Section 1. Earthquakes chosen for the analysis are listed in Table 1, which are deep and intermediate earthquakes which occurred in the region of Japan. The *S* wave data for all of the six earthquakes have been given by Ritsema (1965)[1]. Figures from 8 to 13 show distributions of the compression-rarefaction of the observed *P* waves and the *P*-nodal planes obtained by the least squares method in comparison with the graphical solutions given by Ritsema (1965), where throughout these figures the lower half of the focal sphere is projected on the Wulff net after him in contrast with the figures in Section 2. It is noted that data of the compression-rarefaction from reflected *P* waves, *pP*, *PP*, *etc.*, are included in the *P* wave data. It was shown by Hodgson and Adams (1958) that the reflected phases are of poor reliability.

Earthquake of 1934

For this shock Ritsema presented two alternative solutions, that is, a single couple solution and a double couple one. Only six observations of the *S* wave are available to determine a fault plane solution by the method of least squares. The obtained solution, however, surprisingly satisfies the observed *P* wave data, if the small size of the sample is taken into consideration. Figure 8 shows the results and the radiation pattern of the observed *S* wave given by Ritsema, where solid curves indicate the *P*-nodal planes of the L.S. solution and dashed curves correspond to the graphical solution based on the double couple hypothesis after Ritsema. In the figure, the cross of solid lines with the letter, **P** or **T**, indicates the pressure or tension axis for the L.S. solution and the cross of dotted lines that for the graphical solution. The *ESD* is estimated

1) For the case where Ritsema presented two values of the observed polarization angle of the *S* wave at the same station, a mean value of the two is used in the present study.

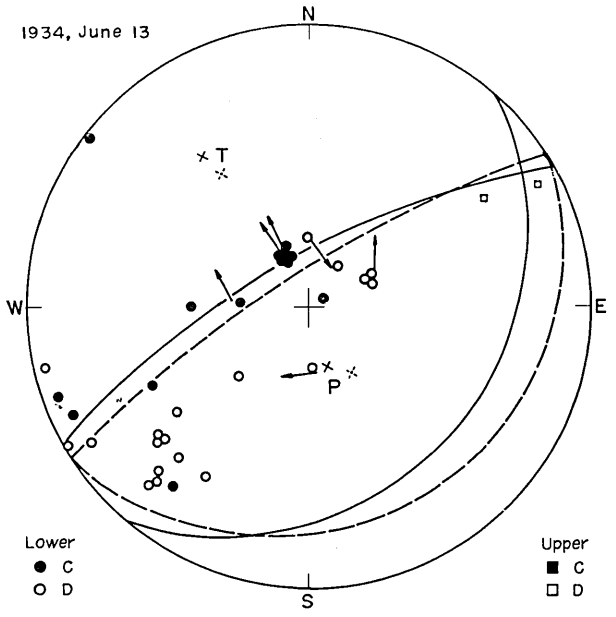

Dip Direc.	Dip
130°.6±17°.4	21°.9±3°.6
-29.8± 3.9	69.2±1.5

Fig. 8. The radiation patterns of the observed P and S waves for the earthquake of June 13, 1934.

For Figures 8 to 13, the observed motion is illustrated by the Wulff projection of the lower hemisphere (after Ritsema; 1965), where solid curves correspond to the least squares solution and dashed curves to the graphical solution, and solid circles indicate condensations and open circles dilatations as before.

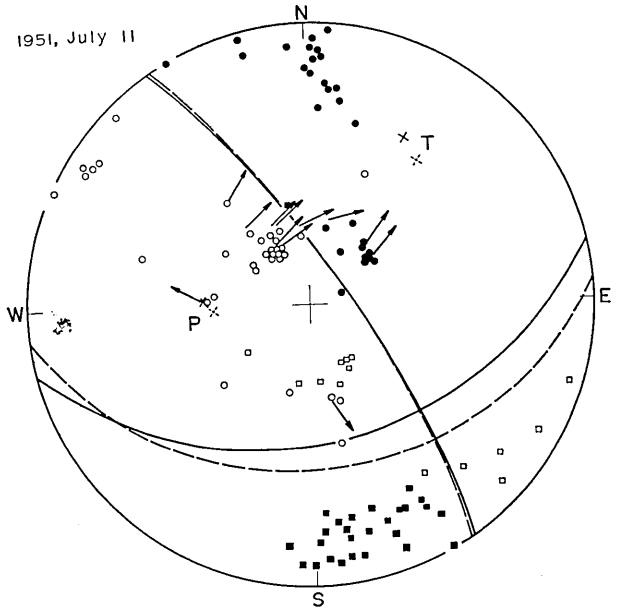

Dip Direc.	Dip
167°.3±5°.9	37°.7±6°.6
55.9±3.0	74.3±2.2

Fig. 9. The radiation patterns of the observed P and S waves for the earthquake of July 11, 1951.

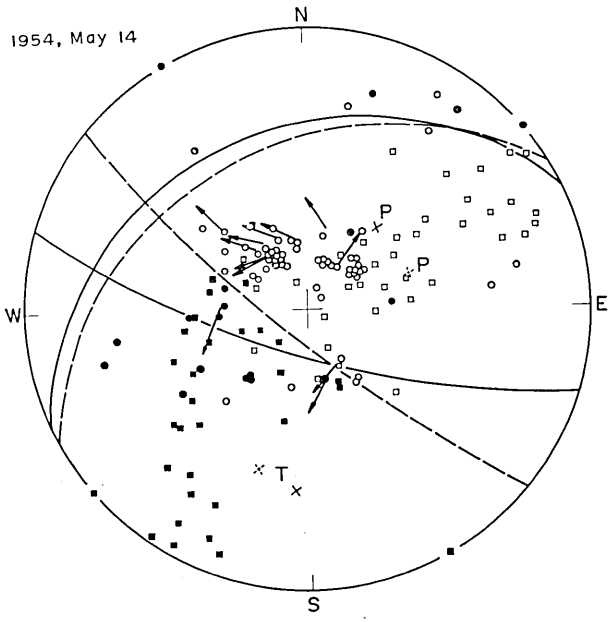

Dip Direc.	Dip
-24°.6±16°.2	25°.2±3°.4
-163.0± 5.9	70.7±1.6

Fig. 10. The radiation patterns of the observed *P* and *S* waves for the earthquake of May 14, 1954.

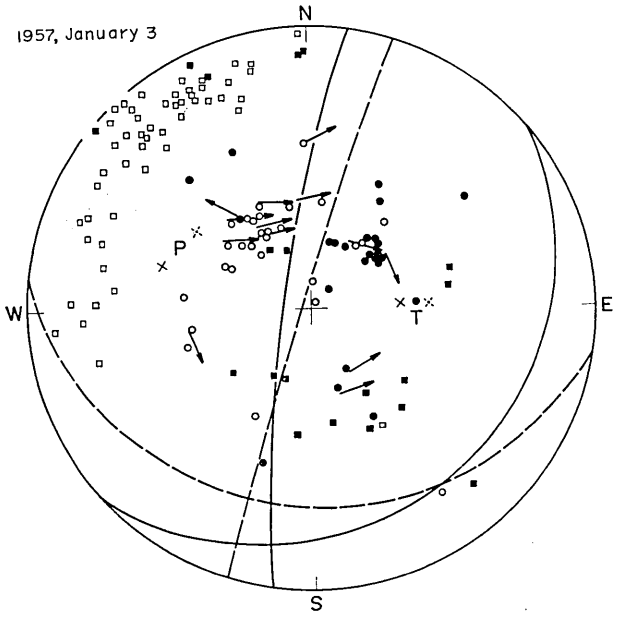

Dip Direc.	Dip
139°.8±22°.5	14°.9±6°.0
-81°.6± 8°.1	78°.7±2°.6

Fig. 11. The radiation patterns of the observed *P* and *S* waves for the earthquake of Jan. 3, 1957.

to be 6°.8. Standard deviations for the most probable values of dip directions and dip angles are also given in the figure.

Earthquake of 1951

The results are presented in Figure 9, where $N=12$ and $ESD=11°.1$. The least squares solution is quite satisfactory for the P wave observations. Especially in respect of the well determined plane of the two P-nodal planes which were obtained visually by Ritsema, agreement between the two solutions is rather surprising.

Earthquake of 1954

In this case two minima of the sum of squares of the residuals are found, where $N=12$. The statistical test by means of the F-distribution shows that difference of estimates of the population variance between the two L.S. solutions is significant. The solution illustrated in Figure 10 is thus adopted as the most probable solution that is determined independently of the P wave observation. The ESD is estimated to be 16.°2. Some inconsistent observations of the P waves with the L.S. solution are seen in the middle of the figure. Most of these observations seem to be observations of pP phase or those of P phase very near the epicenter, since these are originally located on the upper hemisphere.

Earthquake of 1957

The results are shown in Figure 11, where $N=13$ and $ESD=18.°4$. Although deviation of the L.S. solution from the graphical solution is fairly big, the L.S. solution satisfies the P wave observations quite well.

Earthquake of 1960

This shock was used in the first paper as an example for application of the analytical method, where two minima were found. By means of the statistical test the solution given in Figure 12 is adopted as the most probable solution, where $N=15$ and $ESD=15°.3$. The solution will show good agreement with the pattern of observed P wave motion with a few exceptions of minor inconsistent observations.

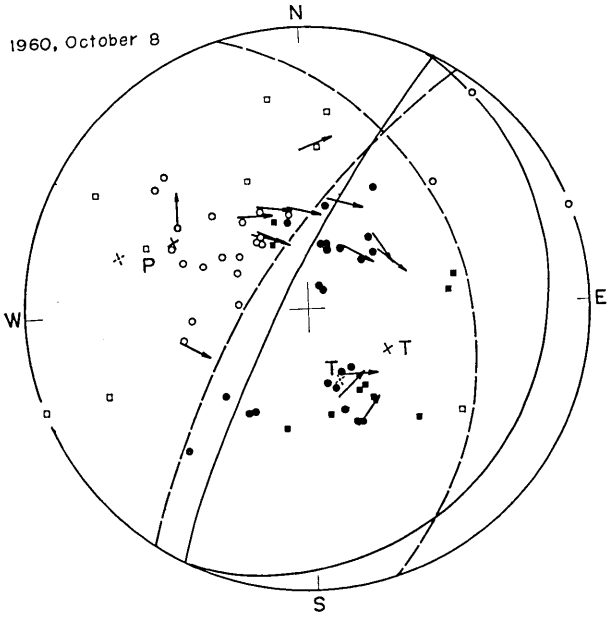

Fig. 12. The radiation patterns of the observed *P* and *S* waves for the earthquake of Oct. 8, 1960.

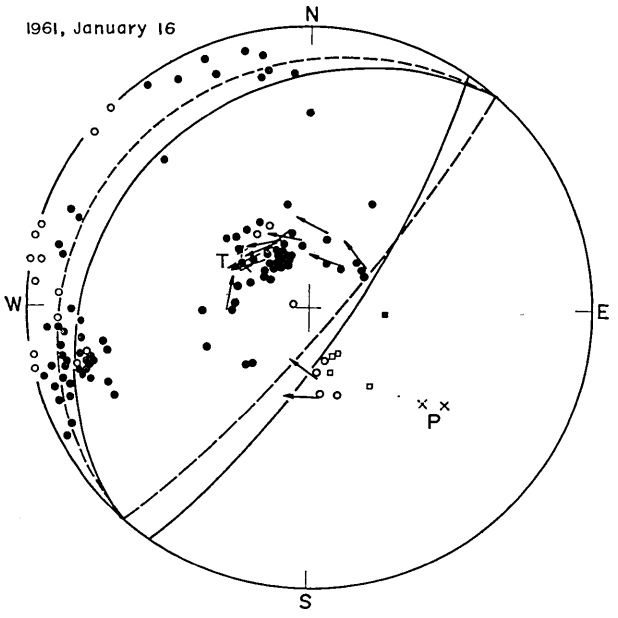

Fig. 13. The radiation patterns of the observed *P* and *S* waves for the earthquake of Jan. 16, 1961.

Earthquake of 1961[2)]

Two minima are found in this case, where $N=12$ and $ESD=18.°4$, $22.°9$ corresponding to the respective two minima. The statistical test by the F-distribution with the 5% limit of significance does not recognize significant difference between the two estimates of the population variance. So far as only the S wave data is concerned, the two solutions should be taken as the alternatives. With the aid of the P wave data, however, it may be found that the solution with $ESD=18°.4$ is more preferable than the other. The preferred solution is illustrated in Figure 13, while the alternative solution is listed in Table 5 in addition to the former. The solution determined thus uniquely is no longer an independent solution of the P wave data in the strict sense.

As may be seen in the figure, the graphical solution as well as the L.S. solution does not satisfy the P wave observation satisfactorily as was remarked by Ritsema (1965). It is noted, however, that the variation of the angle of incidence with respect to the epicentral distance and to the depth of the focus is rather rapid when the angle is larger than around 90°. It follows that disagreements of the solutions with the P wave observations at nearly 90° of the incident angle may be, at least to some extent, attributed to ambiguity of location of the hypocenter. For this earthquake the Japan Meteorological Agency has given the following hypocentral coordinates which are significantly different from those adopted by Ritsema;

$$36°02' \pm 03'\ N,\ 142°16' \pm 06'\ E,\ H=40\ \text{km},$$
$$07^{h}20^{m}04^{s}.7 \pm 1^{s}.3\ \ (\text{GMT}).$$

It does not seem, therefore, that the L.S. solution is in serious contradiction to the P wave observations.

Fault plane solutions obtained in this section by means of the least squares method are tabulated in Table 5. It may be understood from the figures given in Sections 2 and 4 that the standard deviation for the nodal plane depends greatly on the spatial distribution of observing points on the focal sphere relative to the plane. In all the cases in the present

2) Although Ritsema (1965) has given the observed polarization angle at **STU** in his table, the datum is omitted in the present study, since the observation at **STU** does not seem to be illustrated in his figure and the value may naturally be doubted as being misprinted.

Table 5. Fault plane solutions with standard deviations

		1934, June 13		1951, July 11		1954, May 14		1957, Jan. 3		1960, Oct. 8		1961, Jan. 16			
(N)		6		12		12		13		15		12			
$\left(\sum_j \left(\frac{\partial \Psi}{\partial x_j'}\right)^2\right)$		1.8×10^{-11}		8.7×10^{-10}		5.8×10^{-10}		8.3×10^{-10}		7.4×10^{-10}		2.6×10^{-10}		4.3×10^{-10}	
$\left(\sum_j \varepsilon_j^2\right)$		4.3×10^{-15}		4.9×10^{-12}		1.7×10^{-10}		7.5×10^{-13}		6.0×10^{-15}		2.7×10^{-13}		3.9×10^{-13}	
(x_1')		0.26203		0.75288		−0.42700		0.20364		0.08352		−0.18354		−0.93283	
(x_2')		−0.30519		−0.17007		0.19552		−0.17196		−0.16524		0.21147		−0.04311	
(x_3')		0.76363		−0.33878		1.19688		0.20185		0.20988		−0.33494		−0.00546	
(V_{11})		0.15309		0.68354		0.01103		0.20091		0.09288		0.09744		0.31785	
(V_{22})		1.28691		0.36808		0.27431		0.02665		0.02847		0.07803		0.11597	
(V_{33})		0.75693		0.10036		2.09384		0.02187		0.01215		0.03045		0.01780	
(V_{12})		0.42501		−0.50131		−0.01118		0.00709		0.04433		0.08168		0.05051	
(V_{13})		−0.08232		0.05555		−0.02086		0.00580		0.00119		0.00870		−0.03597	
(V_{23})		−0.47508		−0.04643		0.49984		−0.02037		−0.00859		−0.00731		−0.00965	
S. S. Res in rad^2	(Ψ)	0.04249		0.33973		0.71994		1.02982		0.85388		0.92370		1.43921	
Variance in rad^2	$(\hat{\sigma}^2)$	0.01416		0.03775		0.07999		0.10298		0.07116		0.10263		0.15991	
Standard Deviation	$(\hat{\sigma})$	6°.8		11°.1		16°.2		18°.4		15°.3		18°.4		22°.9	
Average of Residuals	$(\bar{R})$	−0°.1		−0°.3		−3°.7		−3°.3		4°.4		0°.1		−3°.5	
Nodal Plane (a)	Dip Direc.	130°.6	±17°.4	167°.3	± 5°.9	−24°.6	±16°.2	139°.8	±22°.5	116°.8	±28°.1	−49°.0	±27°.0	2°.6	± 8°.2
	Dip Angle	21.9	3.6	37.7	6.6	25.2	3.4	14.9	6.0	10.5	1.1	15.6	1.3	43.0	6.9
Nodal Plane (b)	Dip Direc.	−29.8	3.9	55.9	3.0	−163.0	5.9	−81.6	8.1	−61.9	5.2	123.9	8.8	93.0	8.3
	Dip Angle	69.2	1.5	74.3	2.2	70.7	1.6	78.7	2.6	79.5	1.1	74.5	1.6	89.7	3.1
Pressure Axis	Trend	162.4	13.0	−86.5	4.8	41.3	5.4	−73.4	7.4	−62.1	4.6	125.5	11.3	127.2	9.0
	Plunge	65.0	0.5	48.7	5.3	60.9	3.2	33.0	2.9	34.5	1.1	29.4	1.5	30.9	3.5
Tension Axis	Trend	−35.3	6.5	30.3	5.0	−175.6	9.3	86.1	16.0	118.4	10.8	−58.8	10.6	−121.4	8.6
	Plunge	23.9	2.1	21.6	3.1	23.9	1.5	55.3	3.0	55.5	1.1	60.5	1.8	31.4	5.6
Null Axis	Trend	57.7	17.3	135.4	10.3	−78.5	3.4	−169.7	26.6	28.1	50.1	34.4	33.7	3.3	11.6
	Plunge	6.7	14.3	33.2	10.7	15.5	7.9	9.6	10.5	0.2	14.1	1.8	16.5	43.0	7.0
Slip Angle	Plane (a)	71.7	15.8	26.2	6.4	51.2	11.2	49.5	24.8	88.7	30.2	83.2	22.5	0.5	4.5
	Plane (b)	82.8	9.5	55.3	11.0	73.6	6.2	80.2	8.9	89.8	15.0	88.1	7.3	47.0	7.0

section, observing points are located in a cluster at the central part of the focal sphere. For such cases the standard deviation of the dip direction is found generally to be larger than that of the dip angle. On the contrary, for the case in which observing points are distributed near both of the two nodal planes as was seen in figures of Section 2, the standard deviation of the dip angle is usually larger than that of the dip direction.

5. Conclusions and Acknowledgements

The method of least squares based on the double couple hypothesis was applied to 9 deep and intermediate earthquakes which took place in the region of Japan. Using 50 observations for the earthquake of 1956, a statistical test shows that the set of the observations may practically be regarded as a sample from a population of the normal distribution, where the observations mean the residuals of observed polarization angles from theoretically expected ones. The frequency distribution of the superimposed sample confirms the above conclusion. It follows that the estimate by use of the least squares method proposed in the previous paper is the maximum likelihood estimate, and that the fault plane solution and its standard deviation given by the method are statistically reliable.

Except for the earthquake of 1961, fault plane solutions of all the other shocks were obtained independently of the P wave observations. For the shock of 1961, two solutions are presented as the alternatives so far as the S wave data is concerned. Agreement of the present solution derived from the S wave data with the P wave observations is striking even for the case where the least squares solution is obtained from only six observations of the S wave. It is concluded, therefore, that the hypothesis of double couple explains satisfactorily the earthquake mechanism.

Every pressure axis of the least squares solutions for the 9 shocks investigated here is consistent in both plunge and trend with that expected from the known distribution of the pressure axes which are oriented systematically in and near Japan (cf. Honda and Masatsuka; 1952).

The author wishes to thank Prof. H. Honda and Prof. T. Asada for their discussions and kind encouragements. He is indebted to Dr. K. Aki who offered valuable advice. He is also grateful to Dr. R. Sato who read the paper in manuscript and provided helpful comments.

References

HIRASAWA, T. and W. STAUDER, S. J.
1964, "Spectral Analysis of Body Waves from the Earthquake of February 18, 1956", *Bull. Seism. Soc. Amer.*, **54**, 2017-2035.

HIRASAWA, T.
1966, "A Least Squares Method for the Focal Mechanism Determination from *S* Wave Data; Part I", *Bull. Earthq. Res. Inst.*, **44**, 901-918.

HODGSON, J. H. and W. M. ADAMS
1958, "A Study of the Inconsistent Observations in the Fault-Plane Project", *Bull. Seism. Soc. Amer.*, **48**, 17-31.

HONDA, H. and A. MASATSUKA
1952, "On the Mechanisms of the Earthquakes and the Stresses Producing Them in Japan and its Vicinity", *Science Reports, Tôhoku Univ., Ser.* 5, *Geophys.*, **4**, 42-60.

HONDA, H.
1962, "Earthquake Mechanism and Seismic Waves", *Geophysical Notes, Tokyo Univ.*, **15**, *Supplement*, 1-97.

HONDA, H., T. HIRASAWA, and M. ICHIKAWA
1965, "The Mechanism of the Deep Earthquake that Occurred South of Honshu, Japan, on February 18, 1956", *Bull. Earthq. Res. Inst.*, **43**, 661-669.

KASAHARA, K.
1963, "Radiation Mode of *S* Waves from a Deep-Focus Earthquake as Derived from Observations", *Bull. Seism. Soc. Amer.*, **53**, 643-659.

RITSEMA, A. R.
1965, "The Mechanism of Some Deep and Intermediate Earthquakes in the Region of Japan", *Bull. Earthq. Res. Inst.*, **43**, 39-52.

STAUDER, W., S. J. and G. A. BOLLINGER
1964, "The *S*-Wave Project for Focal Mechanism Studies: Earthquakes of 1962", *Bull. Seism. Soc. Amer.*, **54**, 2199-2208.

---

48. *S* 波観測から地震のメカニズムを求める最小二乗法：第二報；実例および統計的吟味

東京大学理学部・地球物理学教室　平　沢　朋　郎

第一報で与えられた最小二乗法が，日本付近に起った9ケの稍深発および深発地震に適用された．

著者等（本多，市川，平沢）によって *S* 波の polarization angle の観測値が求められている3ケの深発地震を用いて，残差（観測値と double couple の仮説に基く理論値の差）の母集団が推定された．適合度の検定および，2ケ以上の地震のデータを重ねた標本の累積頻度分布を正規確率紙に描く事により，残差の母集団は正規分布とみなし得る事が示された．すなわち，この方法により得られる推定量は最尤推定量である事が証明された．

S 波の観測から得られた9ケの地震のメカニズムは *P* 波の観測結果を十分に説明する．その事は double couple の仮説の正当化を意味する．